CARBON 47 (2009) 3392–3402

available at www.sciencedirect.com

ScienceDirect

journal homepage: www.elsevier.com/locate/carbon

Molecular dynamics simulations of nanocarbons at high pressure and temperature

*G. Chevrot, E. Bourasseau, N. Pineau, J.-B. Maillet**

CEA, DAM, DIF, F-91297 Arpajon, France

ARTICLE INFO

Article history:
Received 14 May 2009
Accepted 29 June 2009
Available online 10 July 2009

ABSTRACT

A molecular dynamics study of carbon nanoparticles (980 and 10,034 atoms) under high temperature (1000–7000 K) and high pressure (2–45 GPa) has been made using the reactive LCBOPII potential. The most stable structure of the small cluster is onion-like (encapsulated fullerenic) on the whole pressure range, whereas a transition from onion-like to nanodiamond is observed for the big cluster as pressure increases from 2 to 45 GPa. The melting mechanism depends on the structure, initiated in the core in the case of an onion cluster and at the surface for the nanodiamond. A schematic phase diagram is proposed, that takes into account the finite size effects.

1. Introduction

It has been known for more than 20 years and the important work of Greiner et al. that the detonation of CHNO explosives with a negative oxygen balance (e.g. RDX or TNT) produces soots which contain nanodiamonds [1]. Unfortunately, despite an abundant literature on the subject especially in the last decade (see Refs. [2–15] as examples), it is difficult to get a clear idea of the experimental properties of carbon clusters in detonation products. Indeed, the extreme conditions encountered during the detonation (10–40 GPa, 3000-4000 K) prevent experimentalists from performing analysis *in situ*. As a consequence, spectroscopy studies have mostly been realised in post-production and it has been shown these last years that purification techniques and production methods [12] or even microscopic analysis [14] could modify the nanodiamond structure.

However, nanodiamonds are still commonly represented as spherical particles composed of a diamond core embedded in a graphitic shell, with mean diameters between 4 and 6 nm [6]. Their graphitisation has been widely studied, and all authors observed that nanodiamonds transform into nanographite structures called nano-onions [4,10], although for different graphitisation temperatures. Several authors were interested in the phase diagram as a function of the carbon nanoparticles size and admitted that the melting temperature decreases as the cluster size diminishes. Nevertheless, the conclusions of these different studies are not consistent: whereas the authors in Ref. [3,8] observed that the Graphite/Diamond/Liquid triple point is shifted to lower temperatures and higher pressure as the size of the cluster decreases, Yang and Li [15] claimed that the triple point moves to lower temperatures and pressures as the size of the cluster decreases. Then finite size effects on the phase diagram of carbon still remain unclear.

On the other hand, numerical simulations of carbon clusters are difficult and, as a consequence, the calculated thermodynamic properties of nanoparticles are quite disparate. Actually, the papers related to numerical simulations of carbon mostly deal with the graphitisation of the diamond surface [16–20]. Through a study combining RX spectroscopy and DFT calculations, Raty et al. proposed that carbon nanoparticles produced by detonation exhibit a nanodiamond structure [21]. From DFT calculations, Barnard et al. similarly presented the most stable phase as a function of the carbon nanoparticle size in vacuum [22]: fullerene when the diameter

* *Corresponding author:* Fax: +33 1 69 26 70 77.
E-mail address: jean-bernard.maillet@cea.fr (J.-B. Maillet).
0008-6223/$ - see front matter
doi:10.1016/j.carbon.2009.06.061

is lower than ~1.9 nm, diamond when the diameter is between ~1.9 and ~5.2 nm, and graphite for the larger sizes. Nevertheless, those DFT calculations just allow to briefly relax the initial structure (a diamond particle) and it seems to us that they do not allow to point out phase structure changes. Leyssale et al. published an interesting work [23] about classical molecular dynamics simulations of clusters using the REBO potential. Unfortunately, it appears that this potential is not suited to reproduce the graphite structure, and the authors recognised that their conclusions are probably badly affected by the defects of the potential. Finally, Wen et al. presented recently a DFT study of the relative stability of hydrogenated nanocarbons [24], showing that hydrogen atoms make the diamond structure more stable for small clusters (lower than 1060 atoms).

In this study, we are mainly interested in obtaining a clear description of the structural and thermodynamic properties of nanocarbons under detonation conditions. As a consequence, we used molecular dynamics simulations under extreme thermodynamic conditions to perform numerical experiments of carbon nanoclusters in a representative mixture of detonation products. We used the long-range carbon bond-order potential LCBOPII [25] implemented in the STAMP code developed at CEA. LCBOPII provides a good description of a large variety of carbon allotropes under high temperature and pressure [26]. The temperatures (1000–7000 K) and pressures (2–45 GPa) used in our simulations cover a large scope of the conditions generally encountered during the detonation of usual explosives. The cluster sizes (~1000 and ~10,000 atoms) correspond to spherical particles of about 2 and 5 nm in diameter respectively, which is typical of the nanocarbon sizes recovered in detonation products. As nanodiamonds were annealed at different temperatures, we have been able to depict the graphitisation and melting processes. We have also studied the phase stability (nanodiamond versus nano-onion versus liquid) of the carbon clusters as a function of temperature and pressure. We finally depict a schematic phase diagram and highlight the finite size effects.

The paper is organised as follows: first, the methods are briefly described. Then, the results of the simulations and the thermodynamics properties of the clusters are presented, together with an analysis of the relative phase stability. A discussion and conclusions are provided at the end.

2. Methods

2.1. Simulation conditions

All the molecular dynamics simulations have been run in the *NVT* ensemble using the Langevin thermostat with a friction parameter of 10^{14} s^{-1} and a time step of 0.5 fs. We simulated two clusters containing 980 (C_{980}) and 10,034 (C_{10034}) atoms, corresponding to 2 and 5 nm diameters, respectively. Free boundary conditions are used for the simulations in vacuum. For cases where an external pressure is applied, the clusters are immersed in a bath of argon atoms, the pressure in the clusters being transmitted by interaction with the argon atoms. However we do not explicitely control the applied pressure. Instead, simulations are performed in the canonical (N,V,T) ensemble, and the pressure is computed *a posteriori* using the standard virial formulae averaged over the entire simulation box (carbon + argon atoms). Then pressure is not an input parameter of our simulations. The simulation boxes of sizes $35 \times 35 \times 35$ Å^3 for C_{980} and $61.42 \times 61.42 \times 61.42$ Å^3 for C_{10034} are filled with 875 and 1569 argon atoms for C_{980} (low and high pressure respectively) and 7211 for C_{10034} (high pressure only). Three dimensional periodic boundary conditions are used.

The carbon–carbon interactions are modelled with LCBOPII [25], an empirical reactive potential that was specifically developed to model the variety of carbon allotropes (graphite, diamond, liquid,...) under extreme conditions. The argon–argon and carbon–argon interactions are modelled with Lennard-Jones potentials using a cutoff distance of 10.5 Å. The parameters from Ref. [27] are used for the argon–argon interactions. The carbon–argon parameters are computed according to the Lorentz–Berthelot rule with usual parameters for carbon.[1]

The temperature and pressure conditions are chosen to sample the thermodynamic domain of the expansion of the detonation products, corresponding to temperature and pressure ranges of 1000–6000 K and 2–45 GPa, respectively.

The structural informations are obtained by the analysis of the radial distribution functions (RDF) between the carbon atoms. All the RDF functions encountered in this study exhibit well separated first and second nearest neighbor peaks with a distance of 2.0 Å systematically corresponding to a zero in these functions. We have then chosen this distance as a simple geometric criterion for the distinction bewteen atoms sharing a covalent bond or not. This allows us to discriminate between the different degrees of hybridisation of the carbon atoms, generally sp^2 and sp^3. Besides, the instantaneous configurations of the clusters are given with a colour code (online version) corresponding to the degree of hybridisation of the carbon atom (gray for sp^3, blue for sp^2, and red for sp). Only a 6 Å-thick slice is depicted for clarity. The density profiles are computed from the center of mass of the cluster, with bins of 0.1 Å width (tests have been made in order to get rid of the dependence of the results on the bin width). We have also calculated the mean square displacement (MSD) of the carbon atoms to check for their mobility, and in particular we compared the MSD of the core and surface atoms when possible (the discrimination between these atoms is provided by the density profiles).

3. Results

In this part, we present the structural and thermodynamic properties of the clusters C_{980} and C_{10034} under different temperature and pressure conditions. These sizes correspond to diameters of about 2 and 5 nm, typical of the clusters recovered in the detonation products.

[1] Autodock manual at website: http://autodock.scripps.edu.

3.1. C_{980}

3.1.1. *Simulations at low pressure*

A set of simulations has been realised in the range of 1000–6000 K at low pressure. The total simulation time varies from 20 to 200 ps. The initial configuration of the clusters is a sphere of radius 11.0 Å extracted from bulk diamond. During the simulations at 1000 and 2000 K we observed a rearrangement of the surface atoms. Indeed, as shown in Fig. 1, the surface atoms tend to form a shell surrounding the diamond core of the cluster. The analysis of the density profile confirms the existence of a distinct outer shell, well separated from the rest of the cluster and located at a distance of 9.5 Å from the centre of mass. The width of this shell is about 2 Å with a maximum in the distribution located at 10.5 Å. Partial RDFs have been computed separately for core–core and surface–surface atoms and are shown in the same figure, together with those of the reference diamond and graphite structures. As expected, the nearest neighbour peaks of the RDFs of both bulk diamond and core atoms almost coincide, confirming the fact that the structure of the core remains diamond. Inversely, the first peak of the RDF of surface atoms coincides with bulk graphite, showing that surface atoms preferentially adopt a sp^2 hybridisation and a corresponding bond length. The overall structure of the cluster corresponds to the nanodiamonds described in the literature.

When the temperature is increased to 3000 K, a spontaneous structural transformation occurs and the core atoms rearrange to form concentric shells of decreasing radius. This structure, called nano-onion, is shown in Fig. 2 together with the corresponding density profile and RDF. The sp^2 shells are progressively formed from the outside to the inside of the cluster to finally adopt this "onion structure". At 2500 K (not shown here), the carbon nanoparticle adopts an intermediate structure after 100 ps: the size of the diamond core decreases with respect to the 1000 and 2000 K simulations and two outer graphitic shells are formed. As the graphitisation is a slow process [28], this observed structure is probably not stable and may evolve to a complete onion structure for a sufficiently long simulation time (a discussion about phase stability is provided later in this paper). The simulations at 2500 and 3000 K show that the graphitisation progresses from the surface to the core of the nanoparticle, as observed by others in different conditions [4,5,10,11]. Although some authors observed with semi-empirical or *ab initio* simulations that the graphitisation progresses more easily in the (111) crystallographic direction [29,30], our analysis of both trajectories at 2500 and 3000 K did not reveal any preferential direction for the graphitisation process. This may be explained by the fact that the temperature applied here is higher than the transition temperature that is generally observed experimentally in vacuum (~1000 K), and consequently that the thermal energy is sufficient to graphitise any diamond face.

At 3000 K, the first peak of the RDF of the core atoms is equivalent to the one of the surface atoms (Fig. 2), and coincides with the nearest neighbour distance in bulk graphite. The density profile is typical of the onion structure with three well-defined peaks for $r > 3.5$ Å corresponding to three shells composed of sp^2 atoms essentially. The peak corresponding to the inner shell is broader and exhibits several maxima. Indeed, the associated structure appears more defective, probably as a consequence of the high curvature of the shell. The inter-shell distance is found to lie between 2.9 and 3.0 Å, shorter than the one observed experimentally (3.35 Å for a five-shell onion and 3.24 Å for a 10-shell onion [31]). This discrepancy may be explained by the low pressure in the experiments, performed in standard conditions.

At 4000 K, starting from the nano-onion, the core of the cluster transforms into a disordered structure whereas the outer shell remains unchanged. At 5000 K, the outer shell becomes also disordered and the cluster is entirely melted. The results are displayed in Fig. 3. On the density curve at 4000 K, the peak corresponding to the outer shell is still visible, whereas the other peaks corresponding to the inner shells are barely distinguishable, confirming the disappearance of the shell structure. The MSDs have been computed separately for the core and surface atoms over a 100 ps trajectory and are shown in Fig. 3. The surface atoms exhibit a MSD that converges to an asymptote, typical of a solid structure, whereas the MSD of the core atoms increases almost linearly, typical of a liquid structure. Therefore it seems that the melting of the cluster occurs from the centre to the surface. Indeed in the concentric shell structure, the concentration of defects is higher at the centre of the cluster, helping to accomodate the shell curvature that becomes too high to maintain a regular fullerene shell. Then as the temperature is increased, and despite the steric constraints, the atoms located at the centre of the cluster are energetically unfavoured and initiate the melting process. The atoms located at the surface of the cluster form a stable sp^2 solid shell with no diffusive behaviour and remain in their sites at 4000 K. At 5000 K, the density is quite homogeneous and no distinction can be made between the surface and the core atoms, showing the entire cluster is melted. The average MSD exhibits a linear behaviour with time with a diffusion coefficient equal to 0.25 $Å^2$/ps (the relation between the self-diffusion coefficient D and the MSD is: $D = \frac{1}{6}\frac{d}{dt}(MSD)$).

In order to check for the stability of the onion structure at low temperatures, several thermic treatments have been applied. First, the nano-onion obtained at 3000 K has been annealed at 0 K and its enthalpy compared to the one of the nanodiamond in the same conditions. The enthalpy of the cluster at 0 K is given by:

$$H = U + PV \quad (1)$$

where H is the enthalpy, U the internal energy, P the pressure and V the volume. The calculation of the volume of the cluster is not straightforward and details are given in the Appendix. The results are given in Table 1 and show that the enthalpy of the nano-onion is lower than that of the nanodiamond. Moreover, as the temperature increases we anticipate the entropy contribution to favour the onion structure. That may explain the spontaneous transformation from diamond to onion at 3000 K.

Second, we progressively cooled the 5000 K liquid cluster down to 3000 K using two temperature gradients: 250 K/ps and 20 K/ps. In both cases we observed a rearrangement of the atoms into shells, the cluster progressively adopting an onion structure similar to the one obtained at 3000 K. This

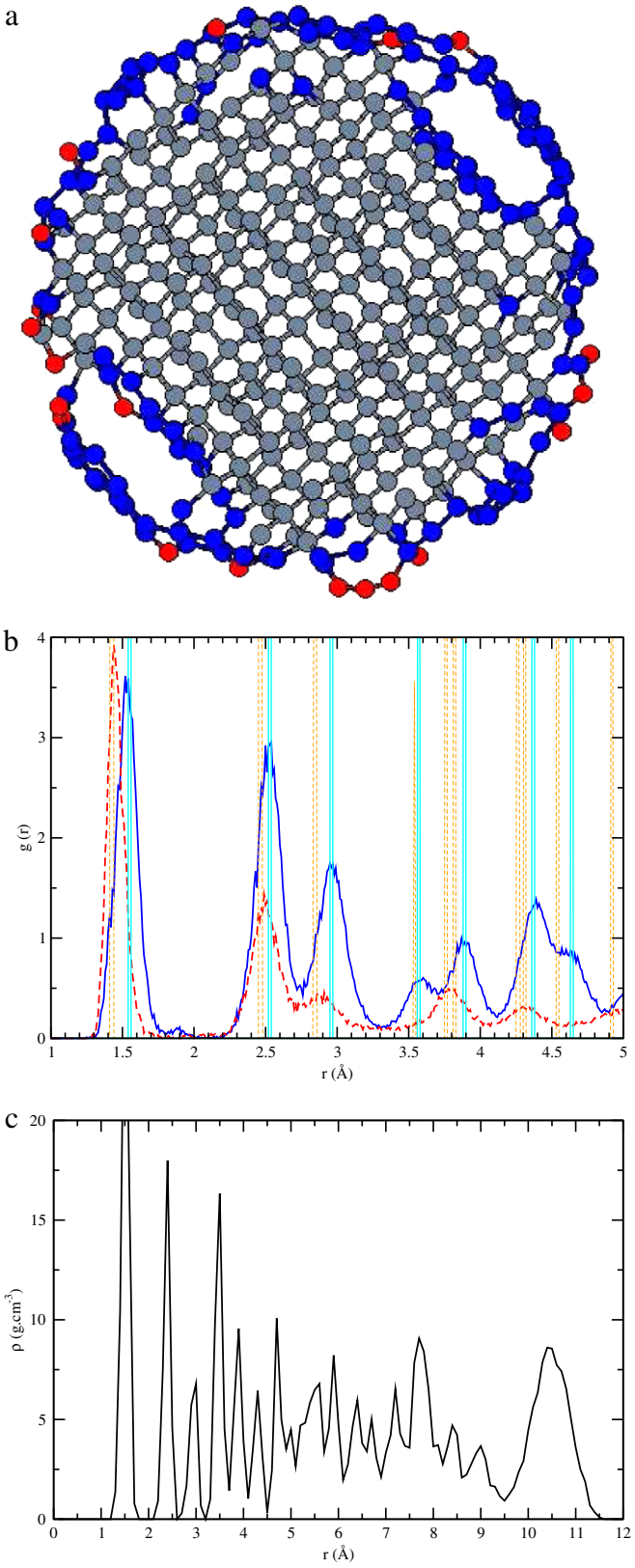

Fig. 1 – (a) Snapshots of the C_{980} cluster at 1000 K. (b) RDF of the core atoms (dark blue curve), the surface atoms (red curve), bulk diamond (blue curve) and bulk graphite (yellow curve). (c) Density profile. (For interpretation of the references to colour in this figure legend, the reader is referred to the web version of this article.)

supports the hypothesis of the stability of the onion structure with respect to nanodiamond. The evolution of the enthalpies of the simulated C_{980} nano-onions and nanodiamonds as a function of temperature are shown in Fig. 4.

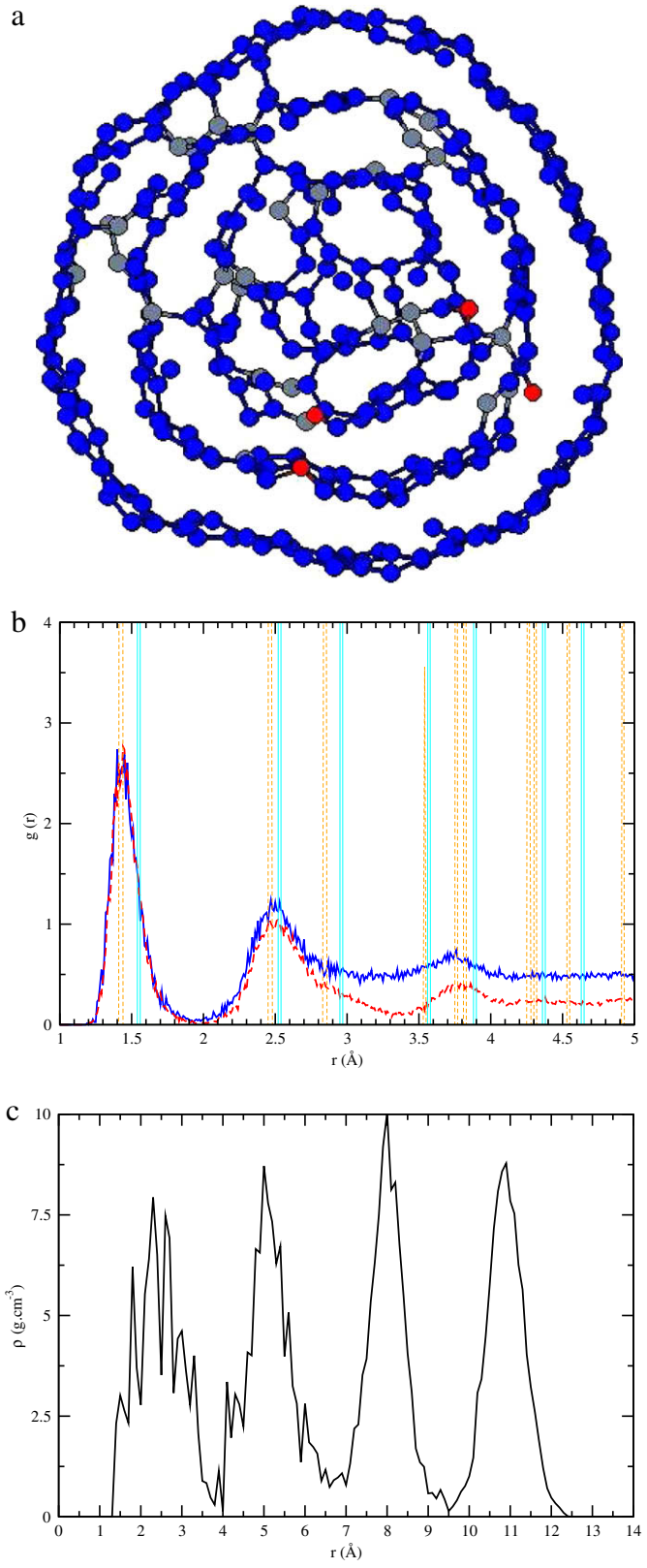

Fig. 2 – (a) Snapshots of the C_{980} cluster at 3000 K. (b) RDF of the core atoms (dark blue curve), the surface atoms (red curve), bulk diamond (blue curve) and bulk graphite (yellow curve). (c) Density profile. (For interpretation of the references to colour in this figure legend, the reader is referred to the web version of this article.)

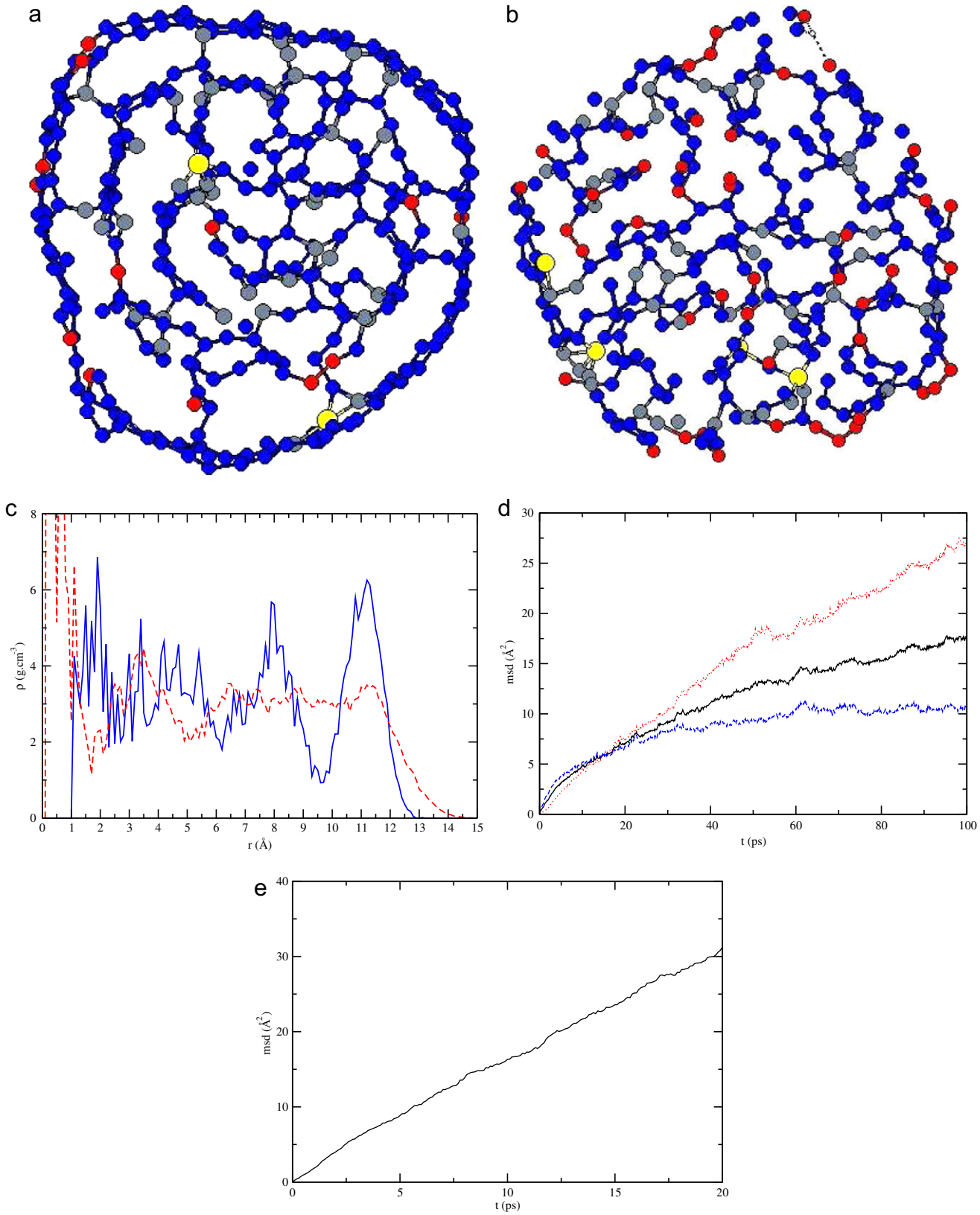

Fig. 3 – (a) and (b) Snapshots of the C_{980} cluster at 4000 and 5000 K. (c) Density curves at 4000 (blue curve) and 5000 K (red curve). (d) and (e) MSD at 4000 and 5000 K (all atoms (black curve), core atoms (red curve) and surface atoms (blue curve)). (For interpretation of the references to colour in this figure legend, the reader is referred to the web version of this article.)

Table 1 – Thermodynamic quantities of C_{980} computed at 0 K.

	Diamond	Onion
U (eV/at)	−6.875	−7.037
P (Pa)	1.44×10^7	7.71×10^7
V (Å^3/at)	7.110	8.065
H (eV/at)	−6.874	−7.033

Therefore the simulations of C_{980} at low pressure (2–9 GPa) shows that the onion structure is the most stable one up to 4000 K. At 4000 K, we observed a partially melted state, with a liquid core surrounded by a solid outer shell. Finally, at 5000 K, the entire cluster is melted.

3.1.2. *Simulations at high pressure*

The simulations at high pressure were performed at 8 different temperatures in the range 1000–6000 K. We observed a similar phenomenology as the one observed at low pressure, i.e. the stability of the onion structure over the diamond one, and only a brief description of the results is given below, with a particular emphasis on the differences with the previous part. The main difference with the behaviour at low pressure is an increase of the graphitisation (or onionisation) and melting temperatures. Previously, starting from diamond, the onion structure was observed to form spontaneously at 3000 K; at high pressure, the onset of this structural transition was observed around 3500 K. Concerning the melting of the cluster, we observed a complete melting at 5000 K in the low pressure case while a temperature of 6000 K was necessary to melt entirely the cluster at high pressure. A similar melting process was observed, starting from the core of the cluster and propagating to the surface.

Similarly to the method used at low pressure, we studied the phase stability of the clusters, particularly between the diamond and onion structures. First we quenched the onion and diamond clusters at 0 K in order to evaluate their respective enthalpies of formation. Once again we found that the onion structure is the most stable one, but with an enthalpy difference lower at high pressure than at low pressure. This is due to the pressure–volume contribution in Eq. 1 because the diamond structure is more compact than the onion structure. Second, we cooled the 6000 K liquid cluster down to 3500 K using the temperature gradients 250 K/ps and 20 K/ps. Upon cooling, the cluster seems to adopt the onion structure, but the transformation remains incomplete, and only the two outer shells are clearly formed, the core being more disorganised. This partial structural transformation is probably due to the limited simulation time but clearly points out the onion structure as the target one.

We finally conclude that the most stable solid structure of C_{980} at high pressure is the nano-onion. The melting mechanism is similar to the one observed at low pressure, i.e. from the core to the surface with a phase coexistence at 5000 K. At higher temperatures, the cluster is liquid.

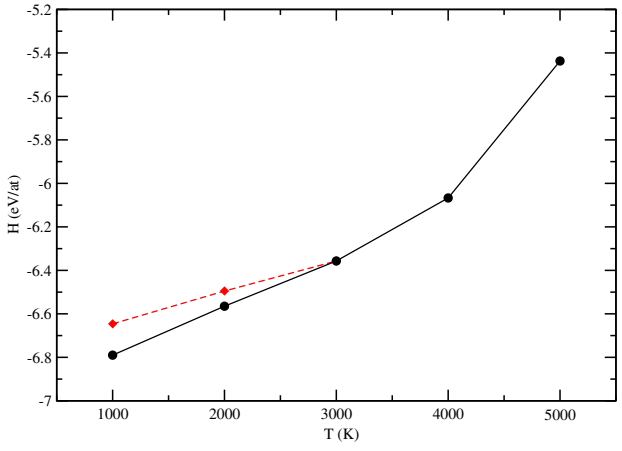

Fig. 4 – C_{980} cluster under low pressure: potential enthalpy (nanodiamond (red diamond) *versus* nano-onion (black circle)) as a function of temperature. (For interpretation of the references to colour in this figure legend, the reader is referred to the web version of this article.)

3.2. C_{10034}

3.2.1. *Simulations in vacuum*

Starting from the diamond structure, we have shown that a small carbon cluster transforms spontaneously into a nano-onion at 3000 K. Nevertheless, this structural transformation is a slow process and may be inhibited by pressure (particularly for larger clusters). Then a set of simulations of the C_{10034} cluster have been performed in vacuum (instead of at low pressure) in order to encourage the appearance of this structural transition in the timescale of our simulations. Results are then presented only in vacuum, and additional simulations at low pressure have not been performed, mainly for CPU time reasons. The initial configuration corresponds to a sphere extracted out of bulk diamond. We have simulated this nanodiamond cluster at 3500 K for 470 ps in order to investigate its structural evolution. A slice of the final configuration is displayed in Fig. 5. Starting from the surface, we observed several onion shells. Nevertheless the shells were less well separated than those observed in the C_{980} cluster. The corresponding density profile shown in Fig. 5 exhibits three peaks corresponding to the three outer shells of the cluster. These peaks overlap and the density remains non-zero between two successive shells, signing the presence of defects in the structure. The density profile of the inner structure is not characteristic of the existence of shells anymore and the associated structure, although based on a sp^2 hybridisation as given by a bond-order analysis, remains rather distorded. The energy profile as a function of the radius (not shown here) confirms that the atoms standing on the outer shells have a lower energy than the core atoms. We think at this stage that the structure of the cluster tends to resemble to the onion structure more than to any other, although the transformation is not complete and the final structure obtained remains defective. Nevertheless, the fact that this structural transition is spontaneous reveals that the diamond structure is not the most stable one at zero pressure.

We tentatively compared the energy of the cluster before the transformation, i.e. in the nanodiamond structure, and after the incomplete structural transformation. We found

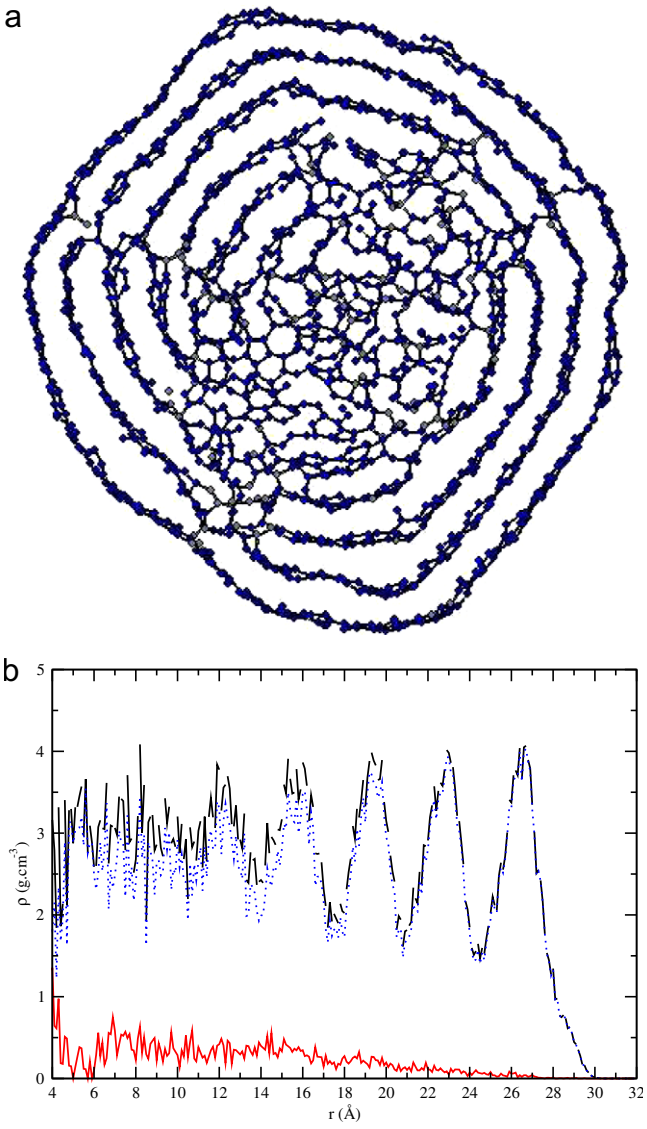

Fig. 5 – (a) Snapshot of the C_{10034} cluster in vacuum at 3500 K. (b) Density curve, total density profile (black), sp^3 atoms (red), sp^2 atoms (blue). (For interpretation of the references to colour in this figure legend, the reader is referred to the web version of this article.)

that the energy of both structures, when quenched at 0 K, are very similar (−7.114 eV/at for the nanodiamond and −7.107 eV/at for the nano-onion). This calculation suggests that the nanodiamond structure is the most stable one, which is obviously not the case here, as the observed structural transition is spontaneous. We think at this stage that the onion structure is the most stable one, as it is the target structure of the spontaneous transition, despite the fact that the simulation time was too short for the transformation to complete. A confirmation of this point was obtained by replacing the core of the incomplete onion cluster C_{10034} by a complete onion cluster of about 2500 atoms that was simulated separately. The new cluster C_{9975}, composed of 9975 atoms, was simulated at 3000 K in order to relax the inter-shell distances, then cooled down to 1000 K and finally quenched to 0 K in order to compare its energy to that of the diamond cluster. Its energy is equal to −7.150 eV/at, thus lower than the one of the diamond cluster confirming the stability of the nano-onion. However, the energy difference between the two structures (0.036 eV/at) remains small.

3.2.2. *Simulations at high pressure*

A set of simulations at high pressure around 30 GPa were performed in the temperature range 1000–7000 K. As already described, during the first picoseconds of simulation at 1000 K we observed the reorganisation of the surface atoms to form a spherical external shell. The atoms of this shell exhibit a sp^2 hybridisation. The core of the cluster keeps a diamond structure. Upon heating, the structure of the cluster remains unchanged up to 4500 K, and no structural evolution toward the onion structure can be detected. At 4500 K, we observed a progressive disorder taking place in the outer shells of the cluster. Indeed, the sp^2 layer is now larger than at lower temperatures and seems less organised. This disordered outer shell is characterised by a high mobility of the atoms and thus analysed as a liquid layer. Along the trajectory, this liquid layer progresses toward the centre of the cluster showing that the melting mechanism of the nanodiamond is different from the one observed for the nano-onion. Indeed, in the case of the nanodiamond, the melting is initiated at the surface of the cluster, where the structure is the most defective. In the case of the small onion cluster, melting is initiated in the core of the cluster, where the structure is the most defective and atoms are the most constrained (due to the high curvature of the inner shell). Then the same cause, i.e. the presence of defects, has different consequences depending on the structure of the cluster.

Although we did not observe any spontaneous transformation to the onion structure up to the melting transition, the stability of the diamond structure over the onion still has to be demonstrated. In order to check the stability of the nanodiamond, we computed the volume associated with both structures under pressure, at around 13 GPa. We found a volume of 8.37 Å^3/at and 6.23 Å^3/at for the onion and for the diamond clusters respectively. This difference in volume contributes to the enthalpy for as much as 0.125 eV/at at 13 GPa in favour of the diamond structure, well above the energy difference between the two structures (evaluated to be lower than 0.1 eV/at). This confirms that the diamond structure is indeed the most stable one for C_{10034} under high pressure.

Our simulations of the C_{10034} cluster have revealed some properties which differ from the C_{980} cluster: at low pressure, the most stable structure seems to be the onion one, as a spontaneous transformation is observed at 3500 K from nanodiamond to a distorded nano-onion. Upon heating, the melting of the onion cluster occurs first in the core and propagates toward its surface, as described in the case of C_{980}. On the contrary, at high pressure, no structural transition is observed and the diamond structure remains unchanged until the complete melting of the cluster, now initiated at the surface and progressing toward the center. An evaluation of the enthalpy of the cluster at high pressure has confirmed the stability of the diamond structure at low temperatures.

4. Discussion and conclusions

4.1. Phase diagram

From the simulation data and the study of the relative phase stability with size and pressure, we can qualitatively depict a phase diagram for both C_{980} and C_{10034} clusters. These are shown in Fig. 6 together with the bulk phase diagram obtained with the LCBOPI+ potential [32] represented in dotted line (yellow coloured online). We can see that the transition line between the graphite and the diamond structure, or equivalently between the onion and the diamond structure in the case of finite size clusters, is shifted to higher pressures as the size of the cluster decreases (from the orange dashed curve for the bulk to the red dotted curve for the small cluster). This shift to higher pressure is clearly a consequence of the finite size effects (i.e. the growing surface over volume ration as size decreases). In the range of pressure of concern for the detonation products (0–40 GPa), we predict that carbon clusters of a thousand atoms do not exhibit a diamond phase. At 0 K, we evaluate a transition pressure close to 43.2 GPa. A model is being developed based on these MD results that allows to compute more quantitatively the coexistence line between the different phases. Moreover, for C_{980}, instead of a melting temperature we rather define a melting range in which we observe a "phase coexistence" between a liquid core and a solid external shell. Although not carefully investigated, we evaluate a 500 K width for this melting range. For temperatures above the melting range, the cluster is entirely liquid.

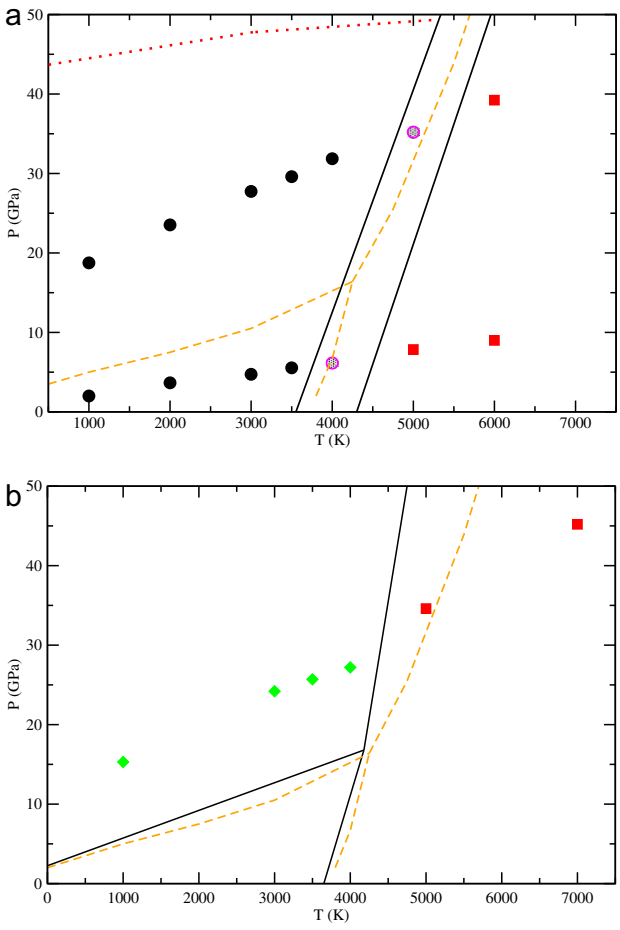

Fig. 6 – (a) Phase diagram of the C_{980} cluster. (b) Phase diagram of the C_{10034} cluster. The separations between the different phases are purely indicative. The graphic points correspond to those obtained in our simulations: nanodiamonds (green), nano-onion (black), quasi-liquid (the core is melted) (purple), and liquid (red). The orange dashed lines correspond to the phase diagram of bulk carbon obtained with the LCBOPI+ potential [32]. The red dotted line corresponds to the NO–ND coexistence line for small clusters. (For interpretation of the references to colour in this figure legend, the reader is referred to the web of this article.)

The case of the C_{10034} cluster is different: although the onion structure is still the most stable one at low pressure, we observe a transition to the diamond structure as the pressure increases. We evaluate a transition pressure close to 2.25 GPa at 0 K, a little bit above the bulk graphite to diamond transition (1.7 GPa [33]), as expected.

The melting temperature was not carefully investigated and is depicted only for clarity. We recall however a change in the melting mechanism as the structure evolves from onion to diamond. Indeed melting is initiated in the core of the cluster in the case of the onion structure whereas it is initiated at the surface of the cluster in the case of the diamond structure.

4.2. Conclusions

The structural and thermodynamic behaviour of carbon clusters of 980 and 10,034 atoms has been investigated through molecular dynamics simulations. The thermodynamic regime of interest is the one of the detonation products of carbon rich explosives, which corresponds to a temperature range of 1000–6000 K and a pressure range of 2–50 GPa. We have shown that at low pressure, the carbon clusters adopt an onion structure, regardless of their size. This structure is seen as the finite size counterpart of the bulk graphite. As the temperature increases, melting is initiated in the core of the cluster, which corresponds to the most defective zone, and occurs on a finite temperature range. In comparison with the bulk phase diagram, the transition line between the onion and the diamond structure is shifted to higher pressures than the graphite to diamond transition when the cluster size decreases. For C_{10034} we evaluate a transition pressure close to 2.25 GPa at 0 K.

Work is in progress to determine more carefully the location of the transition lines, and to build a model for the prediction of the phase diagram of the carbon clusters (as a function of pressure, temperature and size) directly from microscopic simulation data. The equations of state of the carbon clusters obtained through microscopic analysis will then be used to improve the validity of the thermochemical and Monte Carlo calculations of the equilibrium properties of detonation products containing carbon clusters [34,35].

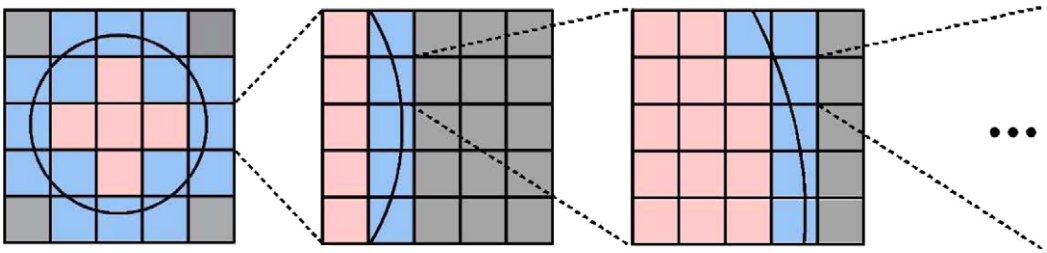

Fig. 7 – Simplified 2D representation of a simulation box containing a carbon cluster (black circle). The box is divided into 5×5 cells. The pink cells contain only carbon atoms and are surrounded by cells containing only carbon atoms. The blue cells contain carbon atoms but are not surrounded by $(3^2 - 1)$ cells containing carbon atoms. The grey cells do not contain any carbon atoms. (For interpretation of the references to colour in this figure legend, the reader is referred to the web version of this article.)

Aknowledgements

Nicolas Desbiens from CEA and Jan Los from ENS-Cachan are gratefully acknowledged for fruitful discussions about methods to calculate cluster volumes. Financial support from the French Agence Nationale de la Recherche (ANR-07-BLAN-0268) is gratefully acknowledged.

Appendix. Calculation of the volume of the cluster

The calculation of the volume of a cluster is not as easy as it could seem. Indeed, in this work, we need to distinguish values of volume close to each other as the thermal expansion coefficient of the clusters is low. As a consequence, the precision obtained on the volume calculation is a very important point.

We tried to apply three methods to get an accurate volume. The first and most obvious one was to get the cluster volume by analysing the density profiles. It is thus possible to estimate an effective radius of the cluster, supposed to be spherical, using the position of the peak corresponding to the last cluster shell in the density profile. Unfortunately, this method gives really poor results when the cluster is not spherical, and is inapplicable when the last shell is not clearly defined. The second approach consists in using an accurate equation of state of argon to obtain the volume occupied by the argon in the simulation box from its pressure. The difficulty here is to measure the pressure of the argon gas: the uncertainty on the pressure calculation, due to the fluctuations of the mechanical equilibrium between the cluster and the gas, leads to an uncertainty up to 10% in some cases.

Finally, we used a more geometrical approach. At first, the box simulation is divided into cubic cells (e.g. $5 \times 5 \times 5$ cells, see a 2D representation of this step in Fig. 7). The cubic cells containing only carbon atoms and surrounded by cells containing only carbon atoms are added to the cluster volume (pink cells in Fig. 7). The cells which do not contain any carbon atom are removed. If a cell contains some carbon atoms but is not surrounded by 26 cells containing carbon atoms, this cell is divided again (blue cells in Fig. 7). To take into account the atomic volumes, the atoms are defined as spheres of radius corresponding to the Van der Waals radius of carbon (1.75 Å [36]). The accuracy of the volume calculation depends on the number of subdivisions. We applied the subdivision process to obtain an uncertainty lower than 1%.

REFERENCES

[1] Greiner NR, Phillips DS, Johnson JD, Volk F. Diamonds in detonation soot. Nature 1988;333:440–2.
[2] Aleksenskii AE, Baidakova MV, Vul A, Siklitskii VI. The structure of diamond nanoclusters. Phys Solid State 1999;41:668–71.
[3] Viecelli JA, Ree FH. Carbon particle phase transformation kinetics in detonation waves. J Appl Phys 2000;88:683–90.
[4] Tomita S, Burian A, Dore JC, LeBolloch D, Fujii M, Hayashi S. Diamonds nanoparticles to carbon onions transformation: X-ray diffraction studies. Carbon 2002;40:1469–74.
[5] Xu NS, Chen J, Deng SZ. Effect of heat treatment on the properties of nano-diamond under oxygen and argon ambient. Diam Relat Mater 2002;11:249–56.
[6] Chen P, Huang F, Yun S. Characterization of the condensed carbon in detonation soot. Carbon 2003;41:2093–9.
[7] Mykhalaylyk OO, Solonin YM, Batchelder DN, Brydson R. Transformation of nanodiamond into carbon onions: a comparative study by high-resolution transmission electron microscopy, electron energy-loss spectroscopy, X-ray diffraction, small-angle X-ray scattering, and ultraviolet Raman spectroscopy. J Appl Phys 2005;97:074302.
[8] Danilenko VV. Phase diagram of nanocarbon. Combust, Expl, Shock Waves 2005;41:460–6.
[9] Larionova I, Kuznetsov V, Frolov A, Shenderova O, Moseenkov S, Mazov I. Properties of individual fractions of detonation nanodiamond. Diam Relat Mater 2006;15:1804–8.
[10] Osipov VY, Enoki T, Takai K, Takahara K, Endo M, Hayashi T, et al. Magnetic and high resolution TEM studies of nanographite derived from nanodiamond. Carbon 2006;44:1225–34.
[11] Qiao Z, Li J, Zhao N, Shi C, Nash P. Structural evolution and Raman study of nanocarbons from diamond nanoparticles. Chem Phys Lett 2006;429:479–82.
[12] Petrov I, Shenderova O, Grishko V, Grichko V, Tyler T, Cunningham G, et al. Detonation nanodiamonds simultaneously purified and modified by gas treatment. Diam Relat Mater 2007;16:2098–103.
[13] Ozerin AN, Kurkin TS, Ozerina LA, Dolmatov VY. X-ray diffraction study of the structure of detonation nanodiamonds. Cristallogr Rep 2008;53:60–7.

[14] Iakoubovskii K, Mitsuishi K, Furuya K. High-resolution electon microscopy of detonation nanodiamond. Nanotechnology 2008;19:155705.
[15] Yang CC, Li S. Size-dependent temperature–pressure phase diagram of carbon. J Phys Chem C 2008;112:1423–6.
[16] De Vita A, Galli G, Canning A, Car R. A microscopic model for surface-induced diamond-to-graphite transitions. Nature 1996;379:523–6.
[17] Jungnickel G, Latham CD, Heggie MI, Frauenheim T. On the graphitization of diamond surfaces: the importance of twins. Diam Relat Mater 1996;5:102–12.
[18] Kern G, Hafner J. *Ab initio* molecular-dynamics studies of the graphitization of flat and stepped diamond (111) surfaces. Phys Rev B 1998;58:13167–75.
[19] Los JH, Fasolino A. Intrinsic long-range bond-order potential for carbon: performance in Monte Carlo simulations of graphitization. Phys Rev B 2003;68:024107.
[20] Wang X, Scandolo S, Car R. Carbon phase diagram from *ab initio* molecular dynamics. Phys Rev Lett 2005;95:185701.
[21] Raty JY, Galli G, Bostedt C, van Buuren TW, Terminello LJ. Quantum confinement and fullerenlike surface reconstruction in nanodiamonds. Phys Rev Lett 2003;90:037401.
[22] Barnard AS, Russo SP, Snook IK. Size dependent phase stability of carbon nanoparticles: nanodiamond versus fullerenes. J Chem Phys 2003;118:5094–7.
[23] Leyssale JM, Vignoles GL. Molecular dynamics evidences of the full graphitization of a nanodiamond annealed at 1500 K. Chem Phys Lett 2008;454:299–304.
[24] Wen B, Zhao J, Li T. Relative stability of hydrogenated nanodiamond and nanographite from density function theory. Chem Phys Lett 2007;441:318–21.
[25] Los JH, Ghiringhelli LM, Meijer EJ, Fasolino A. Improved long-range reactive bond-order potential for carbon. I. Construction. Phys Rev B 2005;72:214102.
[26] Ghiringhelli LM, Los JH, Fasolino A, Meijer EJ. Improved long-range reactive bond-order potential for carbon. II. Molecular simulation of liquid carbon. Phys Rev B 2005;72:214103.
[27] Shashkov AG, Zolotukhina AF, Abramenko TN, Mathur BP, Saxena SC. Thermal diffusion factors for binary gas systems: $Ar–N_2$, $Ar–CO_2$, $He–H_2$, $He–N_2O$, $Kr–N_2O$ and $He–NH_3$. J Phys B 1979;12:3619–30.
[28] Wang C, Chen J, Yang G, Xu N. Thermodynamic stability and ultrasmall-size effect of nanodiamonds. Angew Chem, Int Ed 2005;44:7414–8.
[29] Kuznetsov VL, Zilberberg IL, Butenko YV, Chuvilin AL, Segall B. Theoritical study of the formation of closed curved graphite-like structures during annealing of diamond surface. J Appl Phys 1999;86:863–70.
[30] Barnard AS, Russo SP, Snook IK. Structural relaxation and relative stability of nanodiamond morphologies. Diam Relat Mater 2003;12:1867–72.
[31] Qiao Z, Li J, Zhao N, Shi C, Nash P. Graphitization and microstructure transformation of nanodiamond to onion-like carbon. Scripta Mater 2006;54:225–9.
[32] Ghiringhelli LM, Los JH, Meijer EJ, Fasolino A, Frenkel D. Modeling the phase diagram of carbon. Phys Rev Lett 2005;94:145701.
[33] Bundy FP, Bassett WA, Weathers MS, Hemley RJ, Mao Hu, Goncharov AF. The pressure–temperature phase and transformation diagram for carbon; updated through 1994. Carbon 1996;34:141–53.
[34] Bourasseau E, Dubois V, Desbiens N, Maillet JB. Molecular simulations of hugoniots of detonation products mixtures at chemical equilibrium: microscopic calculation of the Chapman–Jouguet state. J Chem Phys 2007;127:084513.
[35] Hervoudt A, Desbiens N, Bourasseau E, Maillet JB. Microscopic approaches to liquid nitromethane detonation properties. J Phys Chem B 2008;112:5070–8.
[36] Rowland RS, Taylor R. Intermolecular nonbonded contact distances in organic crystal structures: comparison with distances expected from van der Waals Radii. J Phys Chem 1996;100:7384–91.